Proc. of JSCE No. 466/V-19, pp. 121-131, May 1993

# APPLICATION OF MULTI-PHASE MODEL TO THE PIPE FLOW OF FRESH CONCRETE

Kazumasa OZAWA*, Anura S.M.NANAYAKKARA**
and Koichi MAEKAWA***

This paper is to propose the mechanical modeling in terms of the collisional and frictional interaction of constituent particles for flowing fresh concrete through pipelines. The multi-phase formulation was adopted as the basis of computing the resistant force to the deformation arising in tapered and bent pipes. The effect of cement paste existing in fresh concrete on the particle interaction of sands and gravels was taken into account. Approximately 20 different mixtures of concrete were examined for verification of the numerical modeling. The analytical model was proved to be versatile to wider variety of fresh concrete having 3-27 cm by slump and any type of deformed pipe unit with different dimensions. It was emphasized that the pump pressure of concrete being driven through the deformed pipe units can be predicted well chiefly by the particle interaction model of aggregates and the multi-phase scheme.

***Key Words*** : *multi-phase flow, pumpability, fresh concrete, pipeline, deformability*

## 1. INTRODUCTION

The recent demand of high grade fresh concretes is the urgent matter of engineering to rationalize the concrete construction, especially under the latest social background of Japan[1]. Hence, the unified approach to the mechanics of fresh concrete is needed to make the versatile material design and development possible. The high performance concrete[2], which is self-placeable despite the complexity of arrangement of reinforcement and highly durable at hardened stage, is regarded as one of targets to be approached by the advisable mechanics concerned.

The authors have sought the multi-phase model for pipe flow of fresh concrete composite and examined what sort of behaviors the numerical approach could cover concerning the deformation of fresh concrete in shear produced at the tapered and bent pipe units qualitatively[3]. Here, the concept of partial stress was newly introduced. This paper aims at proposing the material constitutive models to represent the particle-to-particle interaction of gravel, sand and cement paste, respectively.

For establishing the relation of the stress versus strain rate for concrete components, we focused on the pressure drop which is necessary to sustain the stable particulate flow through the deformed units of pipes. The flow rate and associated total pressure were measured around those boundary conditions of various dimensions with systematically arranged mixture proportions of fresh concrete[3].

In this study, the deformed pipe units are regarded as the testing apparatus to reproduce the specified mode and intensity for particle-to-particle interaction[6]. The measured pressure is the resultant force generated mainly by the particle interaction and the reaction from the pipe wall. It can be said that the relation of the pressure measured at the inlet of the pipe and the corresponding strain rate, which has been formulated with respect to the rate of flow[4),5], exhibits the stiffness of the particulate flow.

The pump transportation technology of fresh concrete has occupied the indispensable position in recent construction owing to its greater efficiency. The combined pump construction and recent concrete with vast variety of high performance will be realizable in the near future. Hence, it is expected that the multi-phase model for fresh concrete flow and material constitutive models of our great interest will bring the mixture design procedure in terms of the requirement on fluidity, consistency and pumpability. Approximately 40 cases with wide variety of mixtures and the dimensions of deformed pipes were examined for verification of the proposed multi-phase formulation and the particle interaction models of components in concrete.

## 2. GOVERNING EQUATIONS

The authors proposed the general formulation of multi-component solid and liquid phases and verified the performance[3]. Since the detail was reported and cannot be covered within the limited

* Member of JSCE, Dr.Eng., Associate Professor, Department of Civil Engineering, The University of Tokyo (7-3-1, Hongo, Bunkyo-ku, Tokyo 113)
** Member of JSCE, Dr.Eng., Lecturer, Department of Civil Engineering, University of Moratuwa, Sri Lanka
*** Member of JSCE, Dr.Eng., Associate Professor, Engineering Research Institute. The University of Tokyo (7-3-1, Hongo, Bunkyo-ku, Tokyo 113)

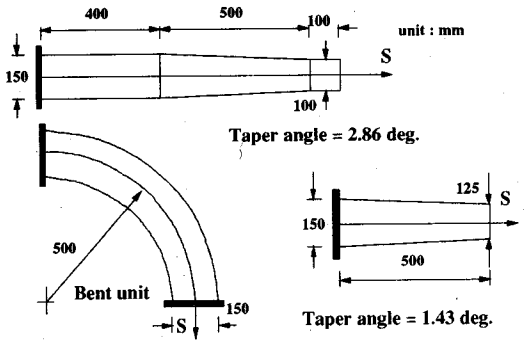


**Fig.1** Analysis target and the coordinate.

space herewith, this chapter summarizes the frame of system formulation. In the scheme of multi-phase formulation proposed, the sectional averaged volume fractions of gravel, sand, powder and water are defined as $C_g$, $C_s$, $C_p$, $C_w$. The volume fractions vary in both time and space domains under the requirement of mass conservation described by,

$$\frac{\partial(AC_i\cdot u_i)}{\partial s}+A\frac{\partial C_i}{\partial t}=0 \quad \cdots\cdots (1)$$

where, $u_i$ is the sectional averaged rate of flow of the assembly of phase "$i$", and the notation "$A$" indicates the cross sectional area defined along the axial coordinate denoted by "$s$" as shown in **Fig.1.**

Regarding four phase system, we must satisfy the following requirement of volume compatibility as,

$$C_g+C_s+C_p+C_w=1 \quad \cdots\cdots (2)$$

For focussing on the segregation between gravel and mortar, we can degenerate the degree of freedom with respect to the speed of phases as,

$$\left.\begin{aligned} &u_w=u_p=u_s(\equiv u_m)\\ &u_g\neq u_m\end{aligned}\right\} \quad \cdots\cdots (3)$$

Other requirement of mechanical dynamics is the conservation of momentum of each phase. The reduction of degree of freedom yields,

$$-\frac{\partial(A\sigma_g)}{\partial s}-2\pi R\tau_g+S_{mg}+\rho_g C_g g_s A=\rho_g C_g A\left(\frac{\partial u_g}{\partial t}+u_g\frac{\partial u_g}{\partial s}\right) \quad \cdots\cdots (4)$$

$$-\frac{\partial\{A(\sigma_s+\sigma_p+\sigma_w)\}}{\partial s}-2\pi R(\tau_s+\tau_p+\tau_w)-S_{mg}+(\rho_s C_s+\rho_p C_p+\rho_w C_w)g_s A=(\rho_s C_s+\rho_p C_p+\rho_w C_w)A\left(\frac{\partial u_m}{\partial t}+u_m\frac{\partial u_m}{\partial s}\right) \quad \cdots\cdots (5)$$

where, $\sigma_i$ and $\tau_i$ are defined on the $i$-phase as the sectional averaged partial normal stress, and peripherally averaged partial shear stress developing at the pipe wall. The value of $S_{mg}$ represents the drag force associated with the segregation of gravel and mortar phases. $\rho_i$ is the net density of particles of $i$-phase, $g_s$, the gravity acceleration in the direction of $s$-axis.

The partial stresses of each phase are composed of the contact stresses generated by the particle to particle interaction of the individual phase concerned and by the stresses applied on the coarser components from the other phases with finer particles as,

$$\left.\begin{aligned} &\sigma_w=(1-C_g-C_s-C_p)\cdot P\\ &\tau_w=(1-C_g-C_s-C_p)\cdot\tau_{cw}\end{aligned}\right\} \quad \cdots\cdots (6\text{-}1)$$

$$\left.\begin{aligned} &\sigma_p=(1-C_g-C_s)\cdot\sigma_{cp}+C_p\cdot P\\ &\tau_p=(1-C_g-C_s)\cdot\tau_{cp}+C_p\cdot\tau_{cw}\end{aligned}\right\} \quad \cdots\cdots (6\text{-}2)$$

$$\left.\begin{aligned} &\sigma_s=(1-C_g)\cdot\sigma_{cs}+C_s\cdot(\sigma_{cp}+P)\\ &\tau_s=(1-C_g)\cdot\tau_{cs}+C_s\cdot(\tau_{cp}+\tau_{cw})\end{aligned}\right\} \quad \cdots\cdots (6\text{-}3)$$

$$\left.\begin{aligned} &\sigma_g=\sigma_{cg}+C_g\cdot(\sigma_{cs}+\sigma_{cp}+P)\\ &\tau_g=\tau_{cg}+C_g\cdot(\tau_{cs}+\tau_{cp}+\tau_{cw})\end{aligned}\right\} \quad \cdots\cdots (6\text{-}4)$$

where, $\sigma_{ci}$ and $\tau_{ci}$ are the contact stresses in sectional averaged compression and shear. The parameter $P$ is defined as pore liquid pressure equal to $\sigma_{cw}$.

The contact stress of each phase can be predicted by the constitutive laws provided that the local strain rate would be derived from the field of flow. The authors manifested the flow field and deformation of dense solid-liquid indicated by,

$$J_g=0 \quad \text{for straigth pipe} \quad \cdots (7\text{-}1)$$

$$J_g=\frac{\sqrt{3}}{R}\cdot\tan\theta\cdot u_g \quad \text{for taper pipe} \quad \cdots\cdots (7\text{-}2)$$

$$J_g=\frac{\phi}{2}\cdot u_g \quad \text{for bend pipe} \quad \cdots\cdots (7\text{-}3)$$

$$\left.\begin{aligned} &J_s=\left(\frac{1}{1-C_g}\right)\cdot J_g\\ &J_p=\left(\frac{1}{1-C_g-C_s}\right)\cdot J_g\end{aligned}\right\} \quad \cdots\cdots (8)$$

where, $J_i$ indicates the sectional averaged second invariant of strain rate of each phase in fresh concrete[4),5),7)].

The values of $R$, $\theta$ and $\phi$ indicate the dimensions of deformed pipes, that is, the radius of the section, the tapering angle and the curvature of the bent pipe. This invariant represents the intensity of shear mode rate of deformation of particle assembly.

According to the experimental results with different tapering angles under the lower rate of flow, the direct proportionality was reported regarding the shear rate[4)] and the particle interac-

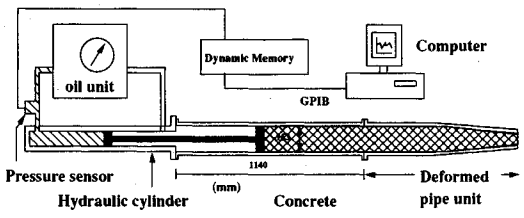


**Fig.2** Experimental set-up for pumping resistance test[6].

tion stress[6]. Then, we have,

$$\left.\begin{aligned}\sigma_{cg}&=K_g\cdot J_g\\ \sigma_{cs}&=K_s\cdot J_s\\ \sigma_{cp}&=K_p\cdot J_p\\ K_p&=0\end{aligned}\right\}\quad\cdots\cdots(9)$$

$$\left.\begin{aligned}\tau_{ci}&=\left(\frac{\mu_i+\theta}{1-\mu_i\cdot\theta}\right)\cdot(\kappa_i\cdot\sigma_{ci}+\theta\cdot\tau_{vi})+\tau_{vi}\\ \tau_{vi}&=\tau_{v0,i}+\eta_i\cdot u_i\end{aligned}\right\}\quad\cdots\cdots(10)$$

where, $K_i$ is the axial stiffness of each phase, and $\kappa_i$ represents the lateral stress ratio as one of constitutive laws. The value of $\tau_{vi}$ is the viscous shear stress composed of the yield stress denoted by $\tau_{v0,i}$ and the viscosity coefficient by $\eta_i$.

The segregation resistance is involved as the phase interaction force. The experiment on the drag force applied to spherical balls brought the following formulation[3),13)] as,

$$\left.\begin{aligned}S_{mg}&=\left(\frac{3AC_g}{4\pi a^3}\right)D_s\\ D_s&=H\cdot a\cdot(u_m-u_g)+a^2T\end{aligned}\right\}\quad\cdots\cdots(11)$$

where, the mean diameter of the particles is defined as "a" and the values of $H$ and $T$ are viscosity parameters to represent the feature of drag force applied to particles.

## 3. MATERIAL MODELS OF FRESH CONCRETE

The pressure needed to sustain the stable flow of fresh concrete around the deformed pipe was measured with the variety of mixture proportions and the dimensions of the pipes[6]. Since the pressure stably obtained can serve to establish the particle interaction model through the multi-phase approach, the authors adopted the experimental cases where the segregation and the associated instability[3] were not observed in terms of the measured pressure. Hence, the computed pressure mainly depends on the interaction models of particles described by Eq.(9) and Eq.(10).

In fact, the yield force and the viscosity for segregation resistance in Eq.(11) were numerically verified not to be influential to the total pressure, if those values are so greater as to avoid the substantial segregation in analysis[3]. In this study, the segregation resistance model is not substantial but the interaction of particles is the main subject to be completed. Then, the greater viscosity and the yield force enough to avoid the segregation were used in computation, actually, $T=3.5$ gf/cm$^2$ and $H=1.0$ kgf·s/cm$^2$.

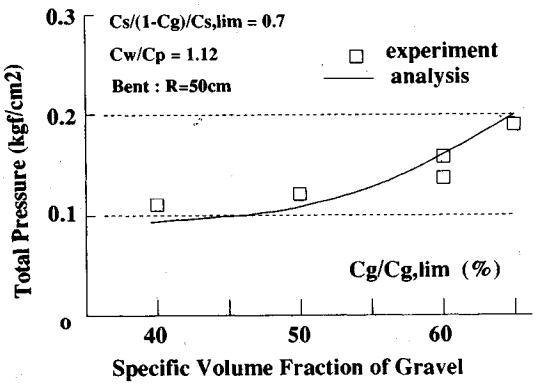


**Fig.3** Total pressure at the inlet of bent pipe with respect to the mixture content of gravel.

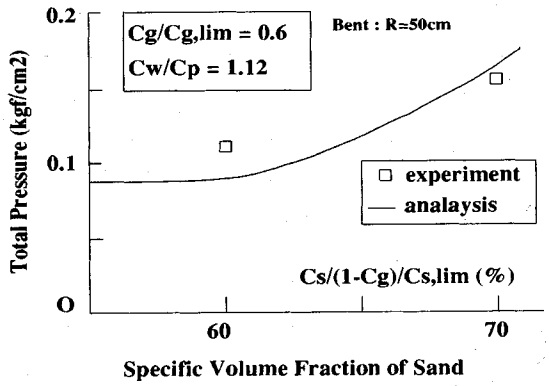


**Fig.4** Total pressure at the inlet of bent pipe with respect to the mixture content of sand.

### (1) Model of Aggregates

As discussed in computational simulation[3], the pressure loss which originates from the deformed pipe units is primarily caused by the aggregates particle interaction. First, the authors focused on different aggregate mixtures with the common water to cement ratio by volume. The experiment to measure the pressure consumed by the deformed pipes were conducted in using pumping resistance test set-up as shown in **Fig.2**[6].

**Fig.3** and **Fig.4** exhibit the total pressure needed to produce the stable flow of concrete in the bent pipe[6]. The flow rate was approximately 5 ±1 cm/s and water to cement ratio by volume was 112%. The parameters changed systematically were specific volume fractions of gravel and sand as

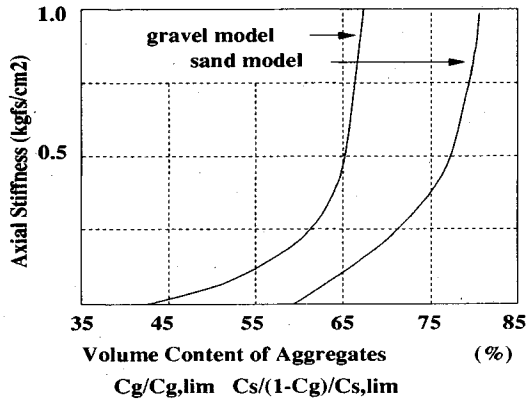


**Fig.5** Assumed stiffness of aggregates with respect to the specific volume fraction of aggregates.

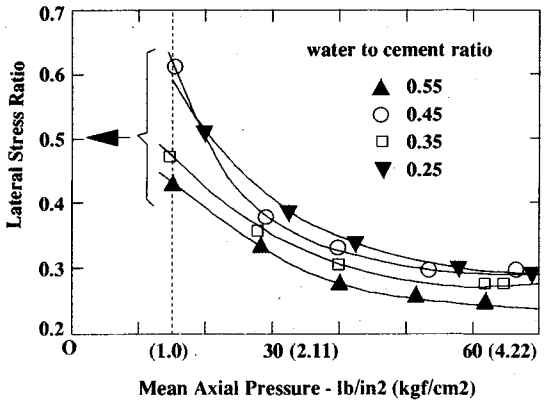


**Fig.6** Variation of the lateral stress ratio of concrete with respect to the mixture and axial pressure[8].

formulated by $C_g/C_{g,\lim}$ and $C_s/(1-C_g)/C_{s,\lim}$ where $C_{i,\lim}$ means the limit compact volume concentration of the $i$-phase. These parameters indicate how densely the aggregates are suspended in the matrix. It was reported that the same pressure drop could be expected when the specific volume fraction would be common no matter what the shape and grading of aggregates are[6].

The authors assumed the stiffness $K_s$ for one particular specific volume fraction of sand $C_s/(1-C_g)C_{s,\lim}$, for instance 70%, and next, they inversely calculated the stiffness for gravel phase in terms of the specific volume fraction as $C_g/C_{g,\lim}$ so that the pressure data of that particular volume contents coincides with the analytical results. Next, using the obtained stiffness of gravel, we checked the pressure data of different volume content of sand under the constant volume fraction of gravel. If good coincidence could not be found, the assumed stiffness of sand was modified until all test results having 112% of the water to cement ratio by volume are fairly predicted.

For analysis, the finite difference scheme[3] was adopted to seek for the simultaneous solution which satisfies the governing equations in Chapter 2. The rate of flow and the volume fractions of each component at the inlet of pipe was the boundary conditions. The analytical solutions in **Fig.3** and **Fig.4** were obtained provided 5 cm/sec of the constant rate of flow at the inlet.

Finally, the authors came up with the stiffness model of aggregates particle assembly based on the experiments of bent pipes as shown in **Fig.5** and formulated by the following equations.

$$K_g\Big|_{\frac{C_w}{C_p}=1.12}=0.14\cdot\tan\left\{5.84\left(\frac{C_g}{C_{g,\lim}}-0.42\right)\right\}\geq 0 \quad \cdots\cdots(12)$$

$$K_s\Big|_{\frac{C_w}{C_p}=1.12}=0.274\cdot\tan\left\{0.58\left(\frac{C_s}{(1-C_g)C_{s,\lim}}-0.59\right)\right\}\geq 0 \quad \cdots\cdots(13)$$

Here, we assumed 0.4 of the frictional coefficient between aggregates and the pipe wall in Eq.(10)[8]. Since the water is non-frictional material whose friction with the solid is independent on the pore pressure, the frictional coefficient of water has to be zero.

The viscous drag stress for aggregates in Eq.(10) must be zero, but the water and powder mixture appears to have some cohesive viscosity. Tanigawa et al. carried out the one-plane direct shear test where the rate dependent and independent stresses were proved. As for the paste shear corresponding to 112% of the water to cement ratio by volume, the typical values were tentatively adopted according to the reference[9] as,

$$\left.\begin{aligned}\tau_{v0,w}+\tau_{v0,p}&=0.8\times10^{-3}\ \mathrm{kgf/cm^2}\\ \eta_w+\eta_p&=0.2\times10^{-4}\ \mathrm{kgf\cdot s/cm^3}\end{aligned}\right\}\cdots\cdots(14)$$

It was reported by Ede[8] that the lateral stress ratio of concrete obtained at the straight pipe varies according to the mixture as well as the mean axial pressure as shown in **Fig.6**. Since there is no lateral deformation along the pipe axis of the bent pipe as in the straight one, it can be assumed that the lateral stress ratio concerning bent pipes is the same as the one for straight pipes. The value of the lateral stress ratio of concrete is approximately 0.5 around the pressure adopted in the series of experiment[6].

Since the stress of fresh concrete is carried by each component as idealized by Eq.(6), the lateral stress ratio of concrete is the resultant value which derives from Eq.(10), Eq.(6) and the specified mix proportion. Then, it cannot be theoretically concluded that the lateral stress ratio of concrete as shown in **Fig.6** does not correspond to the lateral

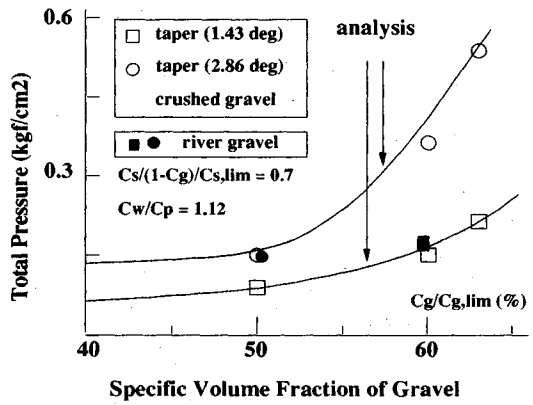


**Fig.7** Total pressure at the inlet of tapered pipe with respect to the mixture content of gravel.

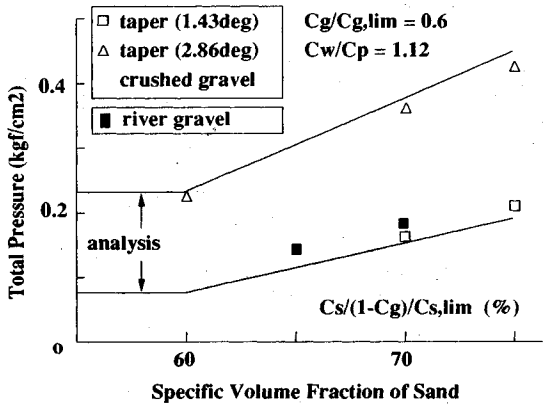


**Fig.8** Total pressure at the inlet of tapered pipe with respect to the mixture content of sand.

stress ratio of aggregates. In fact, when we assume extreme cases where concrete is composed of no solids particles (liquid phase only), the lateral stress ratio must be unity and equal to $\kappa_w$ because of its perfect isotropy.

However, it may be allowed to consider that the measured lateral stress ratio of concrete selected in **Fig.6** will be close to the lateral stress ratio of aggregates as constituent materials of concrete, because the total stress of concrete is carried by the aggregates contact for ordinary mixture of fresh concrete except for the super fluidized concrete. In case of the restriction of lateral displacement, Tangtermsirikul related the local contact friction with the lateral stress factor with the micro contact theorem[10], which shows that 0.5 of $\kappa$ corresponds to 0.33 of the friction coefficient at the particle contact. The computation related to **Fig.3** and **Fig.4** was performed with 0.5 of the lateral stress ratio of aggregates regarding the deformation mode arising in bent pipes.

**Fig.7** and **Fig.8** show the pressure loss produced by the deformation of fresh concrete in tapered pipes[6]. It was clarified that the mode of deformation is pure shear in both tapered and bent pipes, but the direction of the principal axis of deformation in tapered pipe is 45° different from the one in bent units[4),5)]. Since the lateral deformation is agitated by the main axial flow in tapered pipes unlike the bent pipes, comparatively greater lateral stress will be obtained when the particle would be packed so densely, because the particles cannot be easily released in the axial direction of pipes against the axial repulsion by particles' collision. This is not the case of bent pipes in which the principal direction in shear does not coincide with the axial direction of main flow[5], and the lateral stress ratio is thought to have nothing to do with the density of the aggregates. Accordingly, as for the lateral stress ratio for tapered pipes, the authors tentatively proposed the following model which depends on the specific volume fraction of gravel.

$$\left.\begin{aligned} \kappa_g &= 0.2 && \text{for } \frac{C_g}{C_{g,\lim}} \leq 0.5 \\ \kappa_g &= 6\frac{C_g}{C_{g,\lim}} - 2.8 && \text{for } \frac{C_g}{C_{g,\lim}} > 0.5 \end{aligned}\right\} \cdots\cdots (15)$$

Analytical results show good coincidence with the experiments in **Fig.7** and **Fig.8**. The sensitivity of the tapering angles, which is associated with the model of compatibility equation to specify the shear strain intensity concerning the dimension and shape of pipes, can be fairly predicted. The sensitivity of gravel and sand volumes in mixture to the pressure needed is also similar to the reality.

For computation of the pressure loss created by the tapered unit, the same axial stiffness of aggregates as Eq.(12) and Eq.(13) serving bent pipe units were utilized too. For adjusting the analytical results with the reality, we could change both the model of axial aggregate stiffness and the lateral stress ratio for particular pipe unit.

This infinite combination of two models may happen to us owing to the stress and strain fields being degenerated from 3 to 1 dimension. This means that the set of axial stiffness and the lateral stress ratio is to be regarded as the constitutive model of aggregates as a whole. In the frame of 1-dimensional flow analysis, the axial stiffness is intentionally defined as common model to represent the intensity of particle stress transfer in the main flow, and the lateral stress ratio is regarded as the model to represent the different mode of deformation.

### (2) Sensitivity of paste phase model to the deformability

The computation in the previous chapter is just related to the same water to cement ratio. Since the

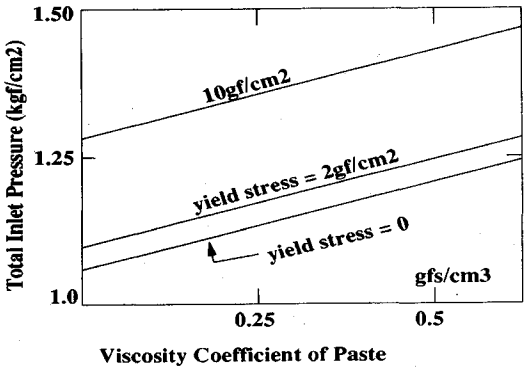


Fig.9 Sensitivity of viscosity coefficient and yield stress as the paste to the total pressure at the inlet of tapered pipe (2.86 deg). : $C_g/C_{g,\lim}=0.6$, $C_s/(1-C_g)/C_{s,\lim}=0.7$, rate of flow=10 cm/s

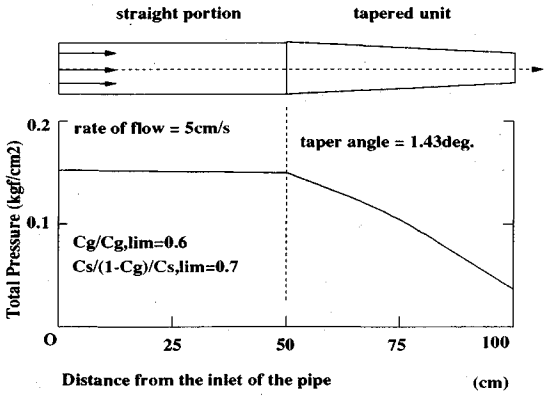


Fig.10 Distribution of the computed axial total pressure along the tapered pipe.

velocities of cement powder and water are assumed common in computation, the change of cement and water mixtures gives rise to the different properties as cement paste. In the above analysis, the typical values for paste wall friction were used as the model of paste in Eq.(14). Since the axial contact stresses of powder and water phases are treated as the hydrodynamic pressure which is not associated with the constitutive law but with the incompressibility and the requirement of compatibility[3], the stiffness model of paste as the constitutive law does not explicitly appear in the frame of multi-phase modeling. Within this study, the effect of cement paste on the drag force at segregation in Eq.(11) is less vital too.

The sensitivity of paste friction model in Eq.(10) to the computed pressure is shown in **Fig.9** with the aggregate model in the previous chapter. The viscosity coefficient and yield stress as the cement paste phase in Eq.(10) vary around 0.01-0.2 gf·s/cm$^3$ and 1-10 gf/cm$^2$ including the standard values in Eq.(14) when the water to cement ratio by weight changes 0.3-0.7 without chemical admixture agent[9]. Accordingly, the paste phase model on friction plays minor role on the pressure at the deformed pipe provided that the segregation would be avoided.

As shown in **Fig.10**, the pressure drop obtained is negligibly small at the straight pipe where the paste friction is the primary source of pressure gradient. This means that the main factor of pressure around the deformed pipes is the aggregate contact within the range of mix proportions as lined up in **Table 1**. This discussion holds if the straight pipe would not be so long as to produce the substantial total pressure loss.

However, the experimental reality is that the mixture in terms of paste has much influence on the pressure loss created by the deformed pipe units[6]. It is impossible to analytically explain the mechanism of paste sensitivity to the pumpability only with the friction model of paste with the pipe wall. The chief source of deformability at the deformed pipes is the particle interaction model described by Eq.(9). It may be reasonable to consider that the mixture of powder and water influences on the particle interaction.

### (3) Interaction model of cement paste and aggregates

Microscopically speaking, the stiffness on contact stress indicates the frequency of collisional events of particles and the effectiveness of stress transfer per one event concerned. Considering that the cement and water (paste) will change the frictional coefficient of contact of aggregates as coarser components, it is reasonable to assume that the aggregate stiffness model be affected by the cement to water ratio of paste between aggregates.

As shown in **Fig.11**, the lower water to cement ratio gives rise to the greater contact friction between solids due to the presence of denser powders which enables higher contact force[11]. In analysis, the interaction between aggregates and cement powder and water is taken into account in terms of the partial stress.

This term represents the effect of stress gradient of finer components on the kinematics of coarser one, such as buoyancy in case of the hydrostatics. Here, the contact stress of coarser components is assumed not to be affected by the presence of finer particles. Then, the change of frictional aspect has to be considered in the model of contact stress.

As far as the frictional behavior of cement is concerned, the similar tendency can be seen in **Fig.12** and **Fig.13** where the sensitivity of water to cement ratio to the total pressure needed is shown[6]. The aggregates were involved with exactly

**Table 1** Experimental Verification

| Test Name | $\frac{C_g}{C_{g,\lim}}$ (%) | $\frac{C_s}{(1-C_g/C_{s,\lim})}$ (%) | $\frac{C_w}{C_p}$ (%) | Powder | Adm. (%) | Slump (cm) | Flow (cm) | Air (%) | Temp. °C | P.exp ($kgf/cm^2$) | Speed ($cm/s$) | Type of pipe | P.cal ($kgf/cm^2$) |
|---|---|---|---|---|---|---|---|---|---|---|---|---|---|
| CMIX5 | 46c | 68 | 126 | C | 1 | 25 | 47x44 | 0.7 | 20 | 0.434 | 5.56 | T2.86 | 0.600 |
| 29MIX6 | 56r | 70 | 89 | CSF | .95 | 22 | 36x39 | 1.5 | 21 | 1.15 | 4.80 | T2.86 | 1.117 |
| 29MIX8 | 49r | 69 | 88 | CSF | .95 | 26 | 59x62 | 2.1 | 20 | 0.547 | 5.26 | T2.86 | 0.623 |
| 30MIX3 | 51r | 73 | 109 | CSF | 1.1 | 24 | 42x43 | 2.2 | 20 | 0.743 | 5.26 | T2.86 | 0.660 |
| 30MIX9 | 53c | 78 | 95 | CSF | .95 | 24 | 43x43 | 1.3 | 19 | 0.791 | 5.00 | T2.86 | 0.967 |
| 30MIX7 | 54c | 70 | 89 | CSF | .95 | 25 | 57x57 | 1.5 | 19 | 0.768 | 5.00 | T2.86 | 0.874 |
| 30MIX8 | 54c | 63 | 84 | CSF | .95 | 26 | 60x59 | 1.1 | 19 | 0.761 | 5.20 | T2.86 | 1.047 |
| BT1 | 50r | 70 | 112 | C | 1.0 | 24 | 38x38 | 2.5 | 16 | 1.569 | 4.00 | B | 1.535 |
| TP2 | 50r | 70 | 112 | C | 1.0 | 25 | 53x54 | 2.5 | 16 | 1.300 | 4.00 | T1.43 | 1.350 |
| 19TP | 50r | 70 | 142 | C | 1.0 | - | 60x60 | 1.8 | 14 | 0.122 | 5.25 | T1.43 | 0.170 |
| 19BB | 50r | 70 | 142 | C | 1.0 | - | 60x60 | 1.8 | 14 | 0.157 | 5.00 | B | 0.210 |
| 22TP2 | 50r | 70 | 122 | C | 1.0 | - | 54x54 | 3.1 | 13 | 0.279 | 5.00 | T1.43 | 0.230 |
| 22BB2 | 50r | 70 | 122 | C | 1.0 | - | 54x54 | 3.1 | 13 | 0.591 | 4.76 | B | 0.320 |
| 25TP | 50r | 70 | 100 | C | 1.0 | 4 | - | 1.5 | 14 | 1.017 | 3.85 | T1.43 | 1.050 |
| 25BB | 50r | 70 | 100 | C | 1.0 | 4 | - | 1.5 | 14 | 1.175 | 4.00 | B | 1.260 |
| 26TP | 60r | 70 | 142 | C | 1.0 | 19 | 40x40 | 2.3 | 11 | 0.708 | 4.00 | T1.43 | 0.716 |
| 26BB | 60r | 70 | 142 | C | 1.0 | 19 | 40x40 | 2.3 | 11 | 0.695 | 3.85 | B | 0.698 |
| 26TP2 | 60r | 70 | 122 | C | 1.0 | 20 | 37x37 | 2.4 | 13 | 0.545 | 4.55 | T1.43 | 0.580 |
| 26BB2 | 60r | 70 | 122 | C | 1.0 | 20 | 37x37 | 2.4 | 13 | 0.790 | 4.35 | B | 0.750 |
| BB1 | 40r | 70 | 112 | C | 1.0 | - | 59x59 | 1.9 | 27 | 0.532 | 5.56 | B | 0.422 |
| BB2 | 50r | 70 | 112 | C | 1.0 | 22 | 40x40 | 1.5 | 28 | 0.594 | 5.26 | B | 0.558 |
| TPB2 | 50r | 70 | 112 | C | 1.0 | 22 | 40x40 | 1.5 | 28 | 0.722 | 5.00 | T2.86 | 0.744 |
| BB3 | 60r | 70 | 112 | C | 1.0 | 18 | 30x30 | 1.0 | 28 | 0.732 | 5.00 | B | 0.716 |
| BB5 | 65r | 70 | 112 | C | 1.0 | 3 | - | 1.0 | 29 | 0.854 | 3.85 | B | 0.921 |
| BB6 | 60r | 60 | 112 | C | 1.0 | - | 62x62 | 1.0 | 28 | 0.519 | 5.56 | B | 0.425 |
| BB9 | 60r | 70 | 112 | C | 1.0 | 18 | 29x29 | 1.3 | 26 | 0.655 | 5.00 | B | 0.716 |
| TBB9 | 60r | 70 | 112 | C | 1.0 | 18 | 29x29 | 1.3 | 26 | 0.773 | 5.00 | T1.43 | 0.710 |
| TBB10 | 65r | 70 | 112 | C | 1.0 | 5 | - | 2.7 | 27 | 0.951 | 4.35 | T1.43 | 1.130 |
| TBB11 | 60r | 65 | 112 | C | 1.0 | - | 22x22 | 1.0 | 23 | 0.636 | 5.00 | T1.43 | 0.550 |
| BB11 | 60r | 65 | 112 | C | 1.0 | - | 22x22 | 1.0 | 23 | 1.022 | 5.00 | B | 1.022 |
| TP | 60c | 70 | 112 | C | 1.0 | 13 | - | 2.5 | 22 | 0.717 | 5.00 | T1.43 | 0.710 |
| TP3 | 60c | 70 | 112 | C | 1.0 | 13 | - | 2.5 | 22 | 1.665 | 4.55 | T2.86 | 1.767 |
| TP4 | 60c | 75 | 112 | C | 1.0 | 16 | - | 2.2 | 21 | 0.970 | 5.00 | T1.43 | 0.890 |
| TP5 | 60c | 75 | 112 | C | 1.0 | 16 | - | 2.2 | 21 | 2.000 | 4.00 | T2.86 | 2.000 |
| TPF1 | 60c | 60 | 112 | C | 1.0 | 21 | - | 1.2 | 21 | 1.049 | 5.00 | T2.86 | 1.070 |
| TPF3 | 60c | 60 | 112 | C | 1.0 | 21 | - | 1.2 | 21 | 0.922 | 4.00 | T2.86 | 0.853 |
| TPS1 | 50c | 70 | 112 | C | 1.0 | - | 64x64 | 2.9 | 23 | 0.390 | 5.56 | T1.43 | 0.330 |
| TPL1 | 50c | 70 | 112 | C | 1.0 | - | 64x64 | 2.9 | 23 | 0.768 | 5.00 | T2.86 | 0.744 |
| TPS2 | 50c | 80 | 112 | C | 1.0 | 11 | 22x22 | 2.0 | 23 | 0.778 | 5.38 | T1.43 | 0.628 |
| TPL2 | 50c | 80 | 112 | C | 1.0 | 11 | 22x22 | 2.0 | 23 | 1.790 | 5.38 | T2.86 | 1.801 |
| TPS8 | 63c | 70 | 112 | C | 1.0 | 19 | 29x29 | 1.9 | 20 | 0.982 | 5.00 | T1.43 | 0.977 |
| TPL8 | 63c | 70 | 112 | C | 1.0 | 19 | 29x29 | 1.9 | 20 | 2.450 | 4.59 | T2.86 | 2.500 |

1) Gravel content : c = crushed gravel, r = river gravel.

2) Powder : C - ordinary Portland cement, CSF - cement(30%) + slag(30%) having Blaine value = $3000cm^2/g$ + fly ash(40%) by weight.

3) Super-plasticizer : dosage specified by the percentage of the weight of powder.

4) Pressure abbreviated by P.exp and P.cal : measured and computed oil pressure in the pump cylinder. The friction between piston and pipe wall and the resistance at the straight portion of the device are deduced. The total pressure applied to concrete is 0.215 times the oil pressure (See Fig.2).

5) BT1 & TP2 : conducted 1 hour after placing concrete in the pump device.

6) Properties of crushed gravel : $C_{g,\lim} = 61.7\%$, $\rho_g = 2.63g/cm^3$, FM = 6.51.

7) Properties of river gravel : $C_{g,\lim} = 64.3\%$, $\rho_g = 2.62g/cm^3$, FM = 6.51.

8) Properties of sand : $C_{s,\lim} = 69.0\%$, $\rho_s = 2.53g/cm^3$, FM = 2.94.

the same amount. Within the range of lower water to cement ratio, the authors assumed the frictional contact modification factor (associated with Zone *B* in **Fig.11**) to the contact stiffness of aggregates by Eq.(12) and Eq.(13) corresponding to $C_w/C_p =$ 1.12 as follows.

$$\gamma_w = \frac{0.45}{C_w/C_p} \exp\left(\frac{0.2}{C_w/C_p - 0.9}\right) \cdots\cdots (16)$$

where, $\gamma_w$ is equal to unity when $C_w/C_p = 1.12$, and empirically specified to get larger than unity when

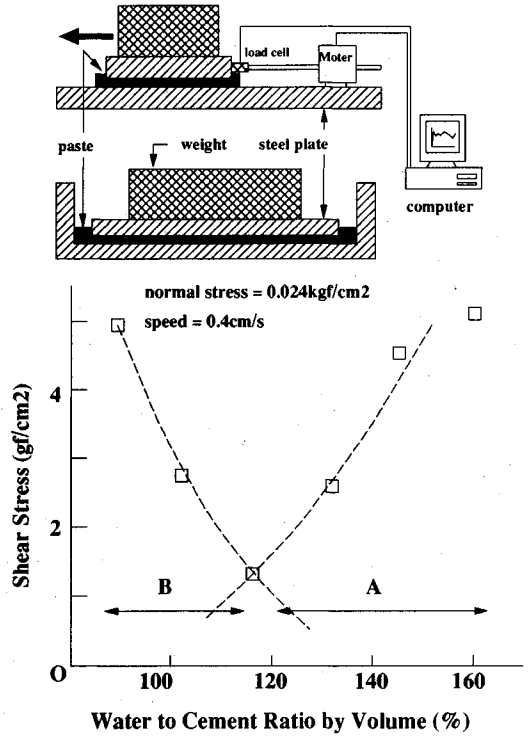


**Fig.11** Frictional stress transfer of paste with different water to cement ratio[11].

water to cement ratio by volume is less than 1.12 as the control value so that we can take into account the higher frictional stress transfer among aggregates through the cement paste having lower water to cement ratio (See Zone *B* in **Fig.11**).

On the contrary, the mechanism of increasing friction is seen in **Fig.11** (Zone *A*) when larger water to cement ratio is assumed in turn. Similar behaviors can be observed in **Fig.12** and **Fig.13** for the compact mixture of gravels as 60% of the specific volume fraction. It can be considered that water and cement powders serve as the coating agent to reduce the local roughness of aggregates at the same time. According to **Fig.11**, the following modification factor was introduced concerning how firmly the paste coating would be maintained at the contact of gravel particles.

$$\gamma_v=\left(\frac{10\cdot C_g}{C_{g,\lim}}-5\right)\left(\exp\left\{5\left(\frac{C_w}{C_p}-1.12\right)\right\}-1\right)+1\geq 1 \quad \cdots\cdots (17)$$

where, $\gamma_v$ is equal to unity when $C_w/C_p=1.12$, and empirically specified to get larger than unity when water to cement ratio by volume is greater than 1.12 as the control value so that we can take into account the increasing friction among aggregates through the cement paste having larger water to cement ratio (See Zone *A* in **Fig.11**).

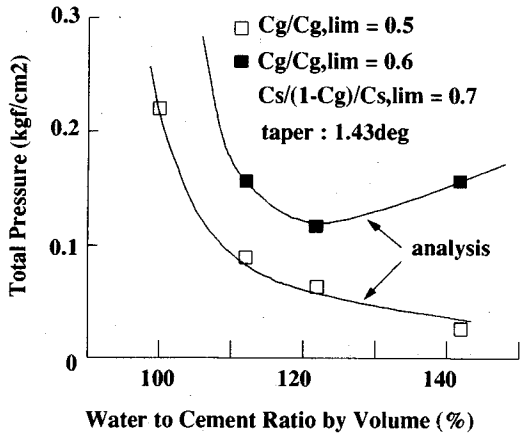


**Fig.12** Calculated total pressure at the inlet of the tapered pipe with respect to the water to cement ratio.

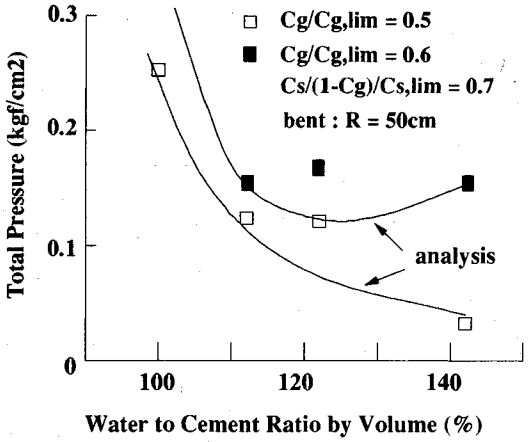


**Fig.13** Calculated total pressure at the inlet of the bent pipe with respect to the water to cement ratio.

In Eq.(17), the specific volume fraction of gravel is included as a parameter since the closer distance between gravels is thought to reduce the cohesive stability of paste around the aggregates[14]. This facet can be also observed in **Fig.12** and **Fig.13**. Through the try-and-error procedure, the authors finally propose the following empirical contact stiffness models which incorporate the volume fractions of aggregates and nonlinear frictional aspect of ordinary cement paste existing in the voids of aggregates as,

$$K_g=\gamma_w\cdot\gamma_v\cdot K_g\big|_{\frac{C_w}{C_p}=1.12} \quad \cdots\cdots (18)$$

$$K_s=\gamma_w\cdot K_s\big|_{\frac{C_w}{C_p}=1.12} \quad \cdots\cdots (19)$$

It is guessed that according to the varying water to cement ratio, the lateral stress ratio might be changed too. Although no experimental data which proves the varying lateral stress ratio is available, it is reasonable to consider that the lateral stress ratio

is associated with the axial stiffness of contact, because both models are physically rooted in the particulate contact of aggregates under deformation. Here, let us define the fictitious volume fraction of gravel denoted as $C_{g,eq}$ which is equivalent to $C_w/C_p=1.12$ as standard. In fact, the fictitious volume fraction can be mathematically obtained by solving Eq.(20).

$$K_g|_{\frac{C_w}{C_p}=1.12}\left(\frac{C_{g,eq}}{C_{g,\lim}}\right)=K_g\left(\frac{C_g}{C_{g,\lim}}\right) \quad \cdots\cdots\cdots\cdots (20)$$

As the lateral stress ratio given by Eq.(15) is applicable to the standard case $C_w/C_p=1.12$, the authors computed the lateral stress ratio by replacing $C_g$ with $C_{g,eq}$. This method implies that the unique relation between the lateral stress ratio of gravel and axial stiffness is assumed, and that the effect of water to cement ratio on both models is postulated to be equable. Shown in **Fig.12** and **Fig.13** for tapered and bent pipes is the sensitivity of the water to cement ratio by volume to the total pressure generated by the flow through the deformed pipes. Analytical model brought the reasonable coincidence with the experiments.

### (4) Experimental verification

Since the above stiffness and factors were defined so that the computation gets equal to the data for particular cases, the other mixtures and their combination with the deformed pipes are required to be verified. **Table 1** includes the analytical results and experiments of 42 cases[6] with concrete mixtures ranging 45-60% of the specific volume fraction of gravel, 63-80% of the specific volume fraction of sand, 84-142% of water to cement ratio by volume, and two types of tapered pipes and one sort of bent pipe. As for powder, the ordinary Portland cement and mixed cementitious powder which was used in high performance concrete[2] were adopted.

**Fig.14** shows the correlation of the computed and the experimental results. Compared with the correlation between the value of slump and the pressure (See **Fig.15**), the computational model is successful. This means that the consistency indicated by the slump test under the gravity is not appropriate for judging the pumpability due to the different boundary conditions and external forces.

**Table 1** also gives the calculated pump oil pressure in using the proposed model. The total sectional averaged pressure at the inlet is 0.215 times the oil pressure according to the difference of the cross-sectional area of piston and the cylinder as shown in **Fig.2**. The coefficient of variation of the calculated to computed pressure ratio is 3.52% and the mean value is close to unity (1.012).

It must be pointed out that the material model on

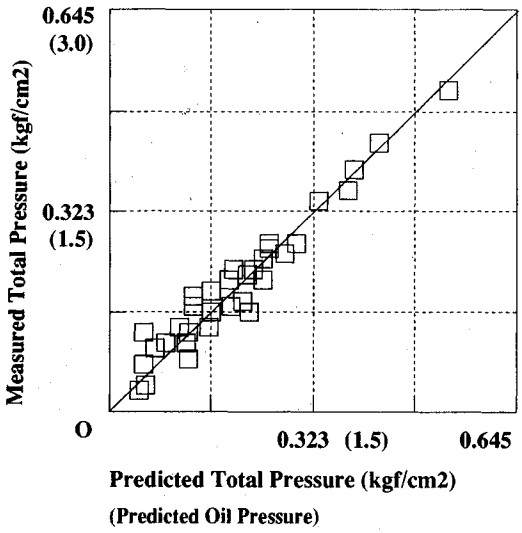


**Fig.14** Comparison of measured and calculated total inlet pressure (pump oil pressure).

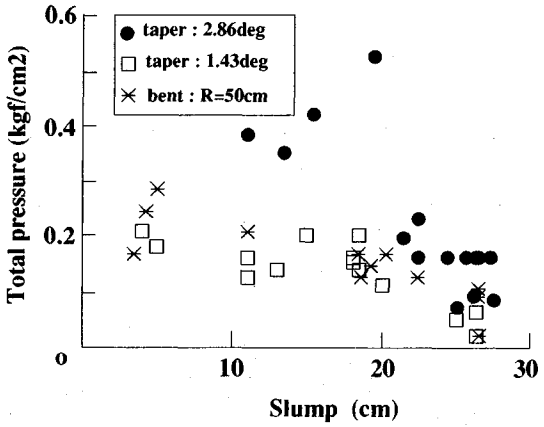


**Fig.15** Relation between slump and the pressure needed to produce the stable flow of concrete.

the effect of cement paste is forceful just under some particular production procedure. Well known time dependent deformability of fresh concrete is not explicitly formulated. The coagulation of powders suspended by water brings the stiffened fresh concrete[12], and in reality, the pumpability was proved being much affected by the time dependent stiffening as shown in **Fig.16**, where one hour after mixing gives rise to approximately three times greater pressure needed at the inlet of tapered and bent pipes.

If the coagulation could be converted to the loss of freely movable water, the elevated pressure has to be computed with some equivalent water to cement ratio, because the loss of the effective free water is to be represented in terms of the water to cement ratio. In computation, the authors took up

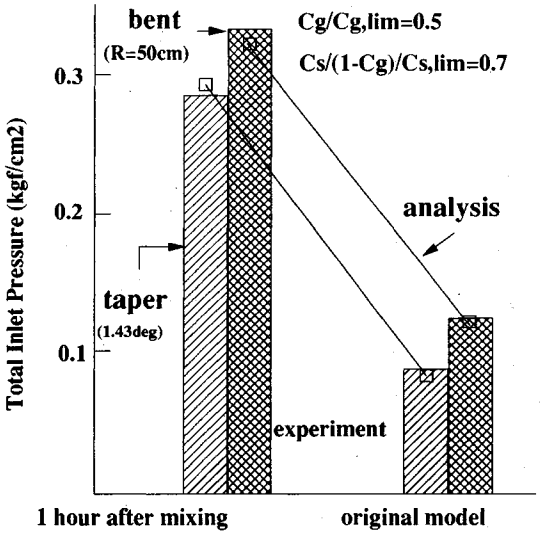


**Fig.16** Elevated pressure by keeping fresh concrete asleep one hour after mixing.

99% of the equivalent water to cement ratio by volume as the alternate of original water to cement ratio (112%) by mixture. As shown in **Fig.16**, for both tapered and bent pipes, analytical results with the equivalent water to cement ratio seems successful. In future, the enhancement of the stress transfer model regarding the cement powder and water system in concrete should be aimed.

Moreover, we should understand that the proposed model can serve only when the ordinary Portland cement is utilized. As reported by the authors[2),6)], the kind of powder can change the feature of stress transfer through particulate friction and collision. Here, let us consider the mixed cementitious powder composed of ordinary cement, fly ash and slag powders. Owing to the spherical shape of fly ash and widely ranging grading of powder phase, internal stress transfer will be reduced in comparison with the single ordinary Portland cement (See **Table 1**). This facet seems to us similar to the case of time dependent hardening of fresh concrete.

**Fig.17** shows the deformational resistance of concrete with mixed sort of powders, which was innovated for special purpose of self-placable concrete having high durability at transient and hardened stages named high performance concrete[2)]. The analytical results as shown in **Fig.17** derived from 112% of the equivalent water to cement ratio based on the ordinary cement as the alternate of the real water to powder ratio (88-89% by volum) with the mixed three sorts of powders. As a matter of fact, the normal cement concrete with $C_w/C_p=88\%$ will be definitely blocked to high resistance to deformation.

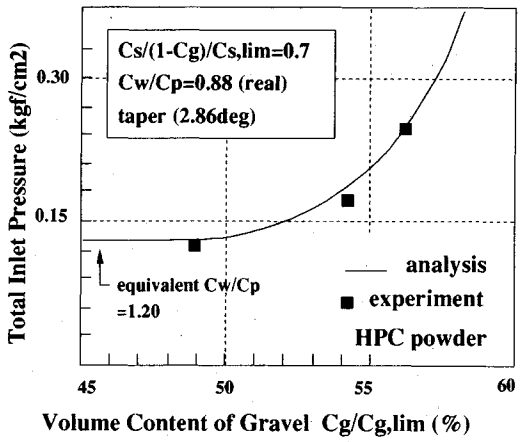


**Fig.17** Predicted total inlet pressure for High Performance Concrete mix proportion.

As discussed above, it is clear that the modeling related to the powder suspension in concrete mixture is crucial for versatility of the predictive method, especially for recent specification of fresh concrete having larger amount of powder. The time dependency of powder suspension and coagulation and sorts of powders have to be generalized in future, if we really seek for the practical usage of the theory. Within the investigation reported in this paper, the aggregates model can be assumed to remain unchanged regardless of time and sorts.

## 4. CONCLUSIONS

Lastly, the authors have to mention clearly that the models proposed in this study are supposed being tentative despite of the well coincidence of analysis with the reality selected in this study. The amount of super plasticizer, the sorts of powders, way of producing concrete and the testing time after mixing were all fixed, and not generally formulated. These factors invariably affect the fluidity and deformational resistance as well as pumpability. Although the role of paste will be investigated in future, the following conclusions can be lined up.

(1) The partial stress concept in line with the multi-phase modeling was verified to be a powerful tool for expanding the applicability of the model to the variety of mixture proportions of concrete.

(2) The stiffness indicating the particle interactions of gravel and sand was found to be different from each other, and influenced by the cement paste. The cement paste may play two roles in fresh concrete, e.g., the matrix suspending aggregates and the agent of frictional stress transfer of coarser aggregates. The water to cement ratio changes the frictional coefficient between solids as well as the stiffness of the matrix itself. Those

aspects were considered in the stiffness model for the contact stresses of aggregates.

(3) The computation was examined by checking various mix proportions, boundary conditions and rates of flow. In spite of the less correlation of the pump pressure with the value of slump, computed pressure as one of indicators of pumpability was proved successful.

The authors attempted the computational approach to the flow of fresh concrete having the features of both solid and liquid. As discussed previously, the modeling was verified close to some particular features of fresh concrete, but somewhat far from the reality at present. No matter how complete the model is, this multi-phase approach could serve as some sort of computerized test of concrete flow and placing without any external vibration in line with the development of self-placable concrete. The segregation under flow was proved an influential factor on the overall workability and pumpability[3]. Herein, the computation exhibited the powerful capability on the way to the development owing to the concept of multi phase which enables us to deal with the variety of mixture proportion and the segregation under flow.

## ACKNOWLEDGMENTS

The authors are grateful to Prof. H. Okamura, The University of Tokyo, for his suggestions and advices granted to them. This study was financially supported by Grant-in-Aid for Scientific Research No.8795443 from the Ministry of Education. The second author extends his gratitude to the Japanese Government for the allocation of Monbu-sho scholarship to him during his academic stay at The University of Tokyo. The last author appreciates the financial support given by JICA to conduct analysis at Asian Institute of Technology.

## REFERENCES

1) Okamura, H. : Waiting for innovation in concrete materials, Cement and Concrete, No.475, pp.2~5, Sept., 1986 (in Japanese).
2) Ozawa, K., Maekawa, K. and Okamura, H. : Development of high performance concrete, Journal of The Faculty of Engineering, The University of Tokyo (B), Vol.XLI, No.3, 1992.
3) Maekawa, K., Ozawa, K. and Nanayakkara, A. S. M. : Multi-phase model for flow of liquid-solid assembly through pipelines, Proc. of JSCE, No.466/V-19, May, 1993.
4) Nanayakkara, A., Ozawa, K. and Maekawa, K.: Deformational compatibility of aggregate phase for tapering flow of dense liquid-solid material, Proc. of JSCE, No.420/V-13, pp.279~290, Aug., 1990.
5) Nanayakkara, A., Ozawa, K. and Maekawa, K.: Deformational compatibility for solid phase of dense liquid-solid flow in bend pipes, Proc. of JSCE, No.426/V-14, pp.221~232, Feb., 1991.
6) Nanayakkara, A., Ozawa, K. and Maekawa, K.: Deformational resistance of fresh concrete through bent and tapered pipes, Proc. of JSCE, No.466/V-19, May, 1993.
7) Ozawa, K., Nanayakkara, A. and Maekawa, K.: Evaluation of aggregate particle motion in liquid-solid flows of model concrete, Proc. of JSCE, Vol.408/V-11, pp.187~193, Aug., 1989.
8) Ede, A. D. : The resistance concrete pumped through pipelines, Magazine of Concrete Research, Nov., pp.129~140, 1957.
9) Tanigawa, Y., Mori, H., Tsutsui, K. and Kurokawa, Y. : Constitutive law and yield criterion of fresh concrete, Proc. of JCI, Vol.9, No.1, pp.115~120, 1988 (in Japanese).
10) Tangtermsirikul, S. and Maekawa, K. : Deformational model for solid phase in fresh concrete under compression, Proc. of JCI, Vol.11, 1989.
11) Izumi, T., Maekawa, K., Ozawa, K. and Kunishima, M. : Influence of paste on the frictional resistance between solids, Proc. of JCI, Vol.10, No.2, pp.309~314, 1988.
12) Hattori, K. and Izumi, K. : A new viscosity equation for non-Newtonian suspensions and its application, Rheology of fresh cement and concrete, E. & F.N. Spon, pp.83~92, 1991.
13) Kishitani, T., Sugawara, T., Oka, S. and Sata, K. : Flowability of fresh cement paste and mortar : Method of measurement, Proc. of AIJ, pp.1022~1023, Sept., 1980 (in Japanese)
14) Powers, T. C. : Properties of fresh concrete, John Wiley & Sons, Inc., 1968.

**(Received, March 26, 1992)**

## 管内を流れるフレッシュコンクリートへの多相モデルの適用

小沢一雅・ナナヤッカラ アヌラ・前川宏一

本研究は，管内を流動するフレッシュコンクリートの挙動を予測するための力学モデルを提案し，その検証を行ったものである．骨材粒子どうしの接触，摩擦による相互作用とそれらに及ぼすセメントペーストの影響を考慮した多相モデルであり，任意の形状のテーパ管やベント管におけるフレッシュコンクリートの圧送抵抗が精度良く予測可能であることが，スランプ3~27 cmの約20ケースのコンクリートを用いた実験により明らかとなった．

土木学会新刊案内

# BASIC Pascal C
## による土木情報処理の基礎 Ⅱ (FD付き)

土木情報システム委員会
教育問題小委員会編

B5版 271ページ 定価 3,800円
会員特価 3,400円 (〒350)

●本書は，次のような方針で編集されています．

- ●卒業研究などで研究室に出入りを始めた学生や，パソコンなどを使用する実務現場に配属された技術者などが，自ら学習しようとするときに役立つテキストとする．
- ●例題は，建設分野に関係のある学生や技術者に親しみやすい内容とする．
- ●すべての例題(全37題)について，パソコン上で動作する4言語(N88-BASIC(MS-DOS版),Quick BASIC, Turbo Pascal, Turbo C) でのプログラム例を，できるだけ同じアルゴリズムで作成して示す．また，プログラム中に詳細なコメントを記述し，読者の理解を助ける．
- ●すべてのプログラムは，その入力データと共に付属のフロッピーディスク(5.25in)に収録して提供する．
- ●巻末付録には，今回対象とした4言語とFORTRAN 77の文法照表を示し，各言語間の相違点を示す．

●本書の構成要素の概要は次の通りです。



本書は，学校や企業の研究室・実験室などで頻繁に発生するデータのハンドリングやアプリケーションプログラムへの入力データの仕様変更，出力からのデータ抽出・グラフ化などの作業を，気軽にコンピュータを使用して行える素養や能力を自ら習得しようとする方々へのよい参考書となると考えていますので，広くご利用ください。

## ■お申込は土木学会刊行物販売係へ

〒160 東京都新宿区四谷1丁目無番地 土木学会 電話03-3355-3441 内線144・145・146 振替東京6-16828
FAX03-3355-3446

# 圧密解析ソフトパソコンに上陸!!

未来設計企業
CRC

## 地盤の非定常圧密解析プログラム

# Mr.圧密

(特長)

- 非定常FEMによる線形弾性解析(christian系の解法)。
- 二次元平面歪解析。
- 要素として三角形・任意四角形が扱える。
- スケーリングをしているので安定して解が求まる。
- リスタート機能の完備。
- 入力はわかりやすいコマンド形式を採用(フリーフォーマット)。
- 図化処理(プロッタ、画像出力)等、豊富な機能を持つポストプログラムを完備。
- ジェネレート機能(長方形要素)により簡単にモデル作成が可能。
- 大モデルはそのままCRCネットワークでも(ホスト処理)可能。

販売価格：60万円　機種：NEC PC9800シリーズ 他

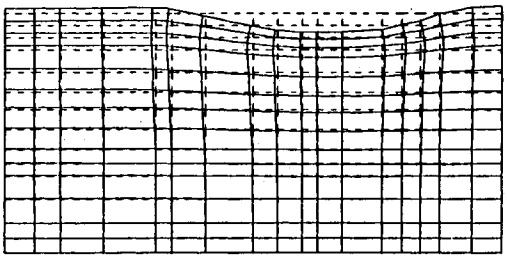

変 形 図

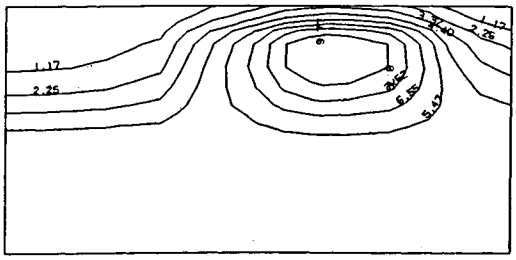


過剰間隙水圧コンター図

※EWS、汎用機用の圧密解析プログラム(逆解析も可能)として"UNICON"も用意しております。

株式会社CRC総合研究所 西日本支社

〒541 大阪市中央区久太郎町4丁目1-3
(06) 241-4121 営業担当:岩 崎
(03)3665-9741 本社窓口:小 林

土木学会論文集

昭和三十七年五月二十八日　第三種郵便物認可
平成五年五月十五日・印刷
平成五年五月二十日・発行
土木学会論文集［四月・四一十日・二十一日発行］

定価1,000円（本体価格・九七一円）